2008

Time Evolution Of Terrestrial Gamma Ray Flashes

Brian W. Grefenstette

David M. Smith

Joseph R. Dwyer

Gerald Jerry Fishman

Time evolution of terrestrial gamma ray flashes

B. W. Grefenstette,[1] D. M. Smith,[1] J. R. Dwyer,[2] and G. J. Fishman[3]

Received 7 December 2007; revised 25 January 2008; accepted 13 February 2008; published 18 March 2008.

[1] We present a study of the time evolution of TGFs observed by both RHESSI and BATSE and compare the data with Monte Carlo simulations of relativistic runaway electron avalanches that record the time of flight for individual photons. Our analysis of the RHESSI data shows that the average delay between the main, hard peak and the secondary, soft tail in the RHESSI data is 28 ± 3 μs. We show that this is consistent with Compton downscattering of hard photons in the atmosphere in our simulations when the source region is located at or below 21 km, which is consistent with previous spectroscopic analysis of the RHESSI data. We also show that the much longer delays (nominally 100 μs) reported for the BATSE TGFs can be understood by the same simulations that are consistent with the RHESSI data once the effects of instrumental deadtime are considered. **Citation:** Grefenstette, B. W., D. M. Smith, J. R. Dwyer, and G. J. Fishman (2008), Time evolution of terrestrial gamma ray flashes, *Geophys. Res. Lett.*, *35*, L06802, doi:10. 1029/2007GL032922.

1. Introduction

[2] Terrestrial Gamma-Ray Flashes (TGFs) associated with thunderstorms were discovered in 1994 by the Burst and Transient Source Experiment (BATSE) on board the Compton Gamma-Ray Observatory (CGRO) [*Fishman et al.*, 1994]. Over the course of its mission, BATSE recorded 76 of the millisecond-duration TGFs. More recent studies of TGFs with the Reuven Ramaty High Energy Solar Spectroscopic Imager (RHESSI) satellite have dramatically increased the number of TGFs observed (over 750 and counting) and the detail of the spectroscopic analysis [*Smith et al.*, 2005; *Dwyer and Smith*, 2005].

[3] An early analysis of a subset of the BATSE LAD data noted a time asymmetry in the TGF lightcurves and the tendency of the TGF spectrum to ''soften'' over time [*Nemiroff et al.*, 1997]. Here we take ''soft'' to mean that more low energy (<300 keV) photons are observed and ''hard'' to mean that more high energy (>300 keV) photons are observed. This softening was later quantified as a time delay between the peak brightness of the hard photons and the peak brightness of the soft photons [*Feng et al.*, 2002]. It was noted that, while TGFs always become softer over time, the time delay between the hard and soft peaks is variable among TGFs, with nominal delays on the order of 100 μs.

[1]Santa Cruz Institute for Particle Physics, University of California, Santa Cruz, California, USA.
[2]Department of Space Sciences, Florida Institute of Technology, Melbourne, Florida, USA.
[3]NASA Marshall Space Flight Center, Huntsville, Alabama, USA.

0094-8276/08/2007GL032922

2. Simulation

[4] In this paper we consider simulations similar to those of *Dwyer and Smith* [2005]. Our model consists of a vertically oriented electric field that drives a relativistic runaway electron avalanche (RREA) process. Bremsstrahlung photons are produced as the runaway electrons stop in the atmosphere after leaving the avalanche region. These photons are then propagated from the emission region through an atmospheric model [*Humphreys*, 1964] to spacecraft altitude (nominally 500 km) by the GEANT3 Monte Carlo package [*CERN Application Software Group*, 1993], which contains all of the relevant physics for the atmospheric processes including Compton scattering, pair production, photoelectric absorption, and the production of secondary electrons and their bremmsstrahlung. The time-of-flight, energy, and lateral distance from the TGF are then recorded.

[5] We consider three source locations at integrated atmospheric depths of 130, 50, and 13 g · cm^{-2}, corresponding to altitudes of 15, 21, and 30 km, respectively. At each source altitude we consider the narrow angular distribution of photons obtained purely from the RREA physics, with the density ($\frac{photons}{sr}$) falling by a factor of two at 16° from the vertical (hereafter, narrow beam), as well as a broad distribution of photons evenly distributed into an upward directed cone with a 45-degree half-angle (hereafter, broad beam).

3. Instruments and Data

[6] Each of the eight BATSE Large Area Detectors (LADs) was a NaI scintillator twenty inches in diameter and half an inch thick as described by *Fishman et al.* [1989]. The LADs were positioned on the eight corners of CGRO so that four detectors would observe a source face on while the other four would observe a source rear on. While data were recorded in many formats, only the Time-Tagged Eventlist (TTE) format had fine enough time resolution (2 μs) and a short enough trigger window (64 ms) to record TGF lightcurves. While the LADs were sensitive to photons with energies from 20 keV to 2 MeV, TTE data were only stored in four fast discriminator channels nominally set to cover the ranges 20–60 keV, 60–110 keV, 110–315 keV, and >315 keV.

[7] The BATSE TGFs were observed serendipitously in the burst mode of the satellite, being mistaken for cosmic gamma-ray bursts. To trigger, an event was required to accumulate enough counts above background during the 64 ms trigger window in a combination of the discriminator channels (http://www.batse.msfc.nasa.gov/batse/grb/catalog/current/trigger_criteria.html). TTE data are available for 36 of the 76 reported TGFs via the public CGRO Legacy archive (ftp://legacy.gsfc.nasa.gov/compton/data/batse/trigger).

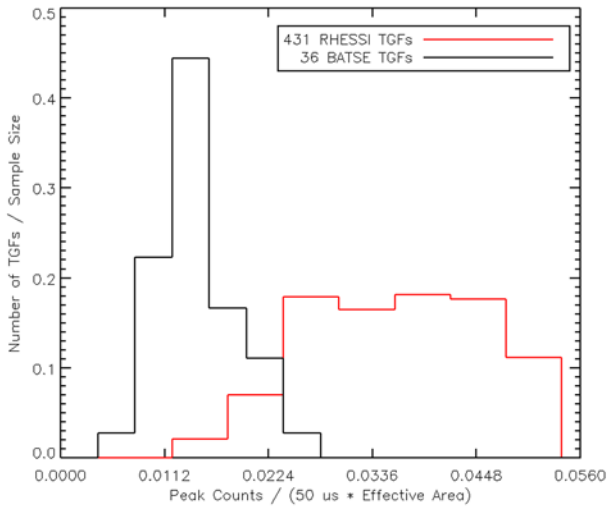

Figure 1. Distribution of peak count rates for all of the TGFs observed by RHESSI (red) and the peak count rates in a single LAD for all of the BATSE events (black). The RHESSI peak rates have been corrected for the deadtime losses as described in the text. The BATSE peak rates have not been corrected for deadtime losses.

We are currently in the process of recovering the remaining events from the original data tapes.

[8] RHESSI's nine germanium detectors observe photons from the entire sky in the energy range 50 keV to 20 MeV as described by *Smith et al.* [2002]. Unlike the onboard trigger of BATSE, RHESSI continuously records every count and transmits the data to ground. Archive data are available from the entire mission and analysis of the RHESSI TGFs is ongoing. We present an analysis of the 431 RHESSI TGFs observed from launch in 2002 through the end of 2004.

4. Instrument Response

[9] We use a standard RHESSI detector response matrix (DRM) that models all 9 RHESSI detectors and the spacecraft, yielding a total effective area of 239 cm^2 for a typical TGF spectrum. The RHESSI electronics are known to exhibit an 8 μs, non-extendable deadtime per observed count. For high count rates in a single detector, the observed signal becomes periodic as the probability of observing an event immediately following the 8 μs deadtime window increases. For low count rates, the arrival times of the counts can be approximated by a Poisson process. Since the distribution of observed delays between counts in all 431 TGFs appears Poissonian we assume that the RHESSI detectors are in the low-deadtime limit and that losses due to the deadtime can be estimated by computing the Poisson probability that a count will arrive in the same detector segment within 8 μs of a previous count.

[10] To construct a DRM for BATSE, we model the average contribution of all eight BATSE detectors as the average of a detector illuminated from the front hemisphere and a detector illuminated from the rear hemisphere. We use GEANT3 and a mass model of an LAD that incorporates all major components of the instrument module (plus an aluminum block to represent spacecraft material) to generate a DRM for both the front and rear detector with effective areas for a typical TGF spectrum of 502 and 160 cm^2, respectively. It has been previously reported that the LADs suffered significant deadtime while observing an extremely bright cosmic gamma ray burst [*Bromm and Shaefer*, 1999]. To investigate whether the LADs are suffering similar effects while observing the much shorter, but brighter, TGFs, we compare the distribution of peak count rates seen by RHESSI, which we assume to be representative of all TGFs, to the peak count rates seen by BATSE.

[11] For the RHESSI TGFs we extract the peak number of counts in a 50 μs bin. To account for RHESSI deadtime we compute the expected fractional loss (f), and find the incident peak count rate (n) from the measured peak count rate (m):

$$n = \frac{m}{1-f} \tag{1}$$

[12] We then scale by the effective area of the combined RHESSI detectors to obtain a peak count rate/50 μs/effective cm^2. For the BATSE TGFs we extract the highest peak count rate in a single LAD for each TGF and scale by the effective area of a front illuminated LAD (Figure 1). Since the BATSE trigger window (64 ms) is much longer than the average duration of a TGF (1 ms) and includes many background counts, we expect BATSE to preferentially trigger on the TGFs with highest peak count rates. We find the opposite result. The peak count rates for the BATSE events are lower than almost all of peak count rates for the RHESSI events. Our interpretation is that the BATSE LADs are suffering from significant deadtime during the peak emission of the TGFs.

[13] The nominal deadtime for the BATSE fast discriminator electronics when observing low energy (<50 keV) photons is two decay times of the NaI fluorescence, or 0.5 μs. However, the fast discriminators are known to present an extendable (paralyzable) deadtime that is dependent on the energy of incident photons. Using pre-flight data (courtesy N. Bhat), we construct a simple model for the

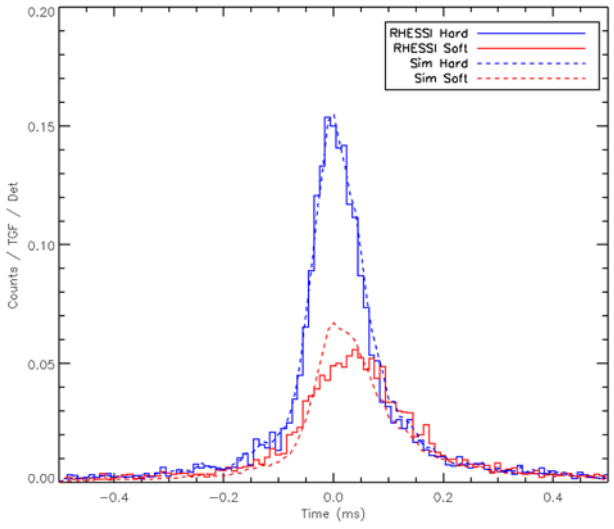

Figure 2. Combined hard (>300 keV, blue) and soft (<300 keV, red) lightcurves for RHESSI (solid) and the broad, 15 km simulation.

Table 1. Hard/Soft Delays[a]

Simulation	Limiting Distance	Delay
15 km Narrow	250 km	17 μs
15 km Broad	450 km	26 μs
21 km Narrow	260 km	16 μs
21 km Broad	490 km	26 μs
30 km Narrow	260 km	10 μs
30 km Broad	530 km	15 μs

[a]RHESSI delay is 28 ± 3 μs.

dependence of the deadtime (τ), in μs, on the energy of an incident photon (2). For a given energy spectrum $\phi(E_\gamma)$, we calculate an effective deadtime $\bar{\tau}$ (3), and then convert between the true count rate (n) and the measured count rate (m) for a paralyzable process [*Knoll*, 2000] (4).

$$\tau(E_\gamma) \approx 0.75 \cdot \log\left(\frac{E_\gamma}{5.5\ \text{keV}}\right) \tag{2}$$

$$\bar{\tau} = \frac{\int \phi(E_\gamma) \cdot \tau(E_\gamma) \cdot dE_\gamma}{\int \phi(E_\gamma) \cdot dE_\gamma} \tag{3}$$

$$m = n \cdot e^{-n \cdot \bar{\tau}} \tag{4}$$

[14] We note that while this correction does not affect the instantaneous spectrum, the overall spectrum of an event may be altered since parts of the event that are harder will experience more deadtime than the parts that are softer. We ignore the long duration (≈10 μs) phosphorescence that occurs when high energy photons deposit large amounts of energy in the scintillator. Such phosphorescence is dependent on the impurities found in each crystal and pre-launch characterizations of the LAD phosphorescence are not available. We consider (2) a conservative estimate of the instrumental deadtime.

5. RHESSI Tails

[15] Since each RHESSI TGF provides too few counts (a median of 20 counts per TGF) to be directly comparable to simulation, we combine the TGFs by using the average times of arrival of the hard counts in each of the TGFs as a common reference. We adjust the times of arrival in a particular TGF to be relative to the average time of arrival of its hard counts and "shift and add" all 431 TGFs into a single, combined event. We correct for the deadtime by collecting the counts into time bins of 10 μs and computing the expected loss fraction (f) in each time bin. We then assign a weight factor for each count in the time bin of $(1\text{-f})^{-1}$.

[16] The delay between the hard and soft components is quantified by comparing the weighted averages of the times of arrival of all of the hard and soft counts. To estimate the uncertainty in this delay, we compute the standard deviation of the mean for each of the weighted distributions and add them in quadrature. We find a delay between the two components of 28 μs ± 3 μs.

[17] To compare our simulations, which represent TGFs with all photons emitted simultaneously, to the data we assume that the time profile of the RHESSI hard counts defines the average time profile of a TGF. We broaden the time profile of the simulations to match that of the data by randomly sampling the distribution of RHESSI hard counts to obtain an initial time offset for every simulated photon.

[18] To compensate for the fact that the combined RHESSI data represents an ensemble of TGFs observed at different distances, we bin the simulated photons into

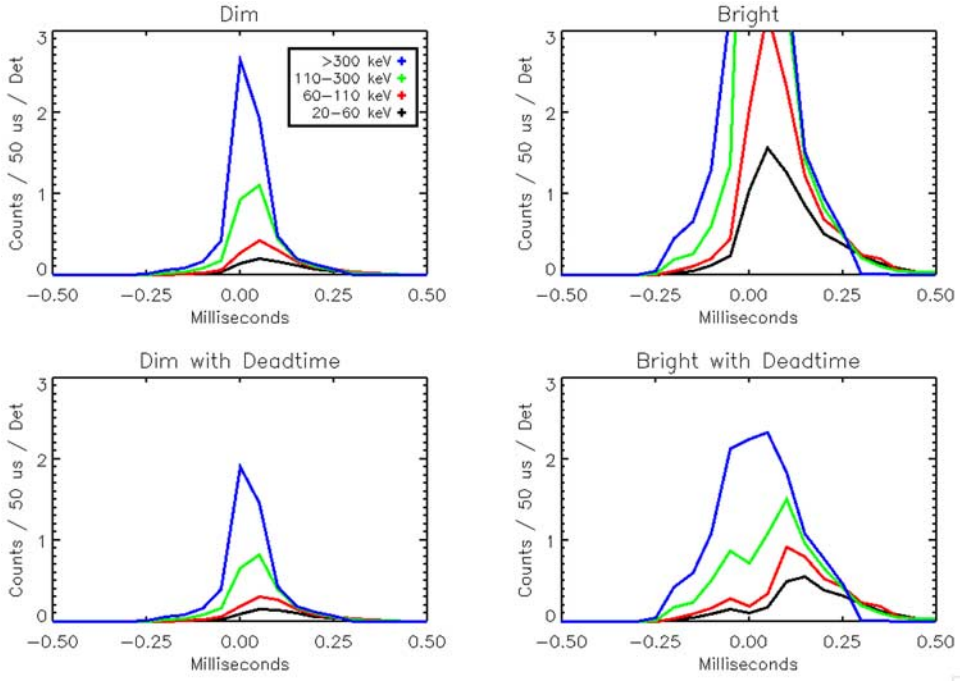

Figure 3. Monte Carlo simulations scaled to the (left) dim and (right) bright RHESSI peak count rates for the broad, 15 km simulation at a distance of 200 km.

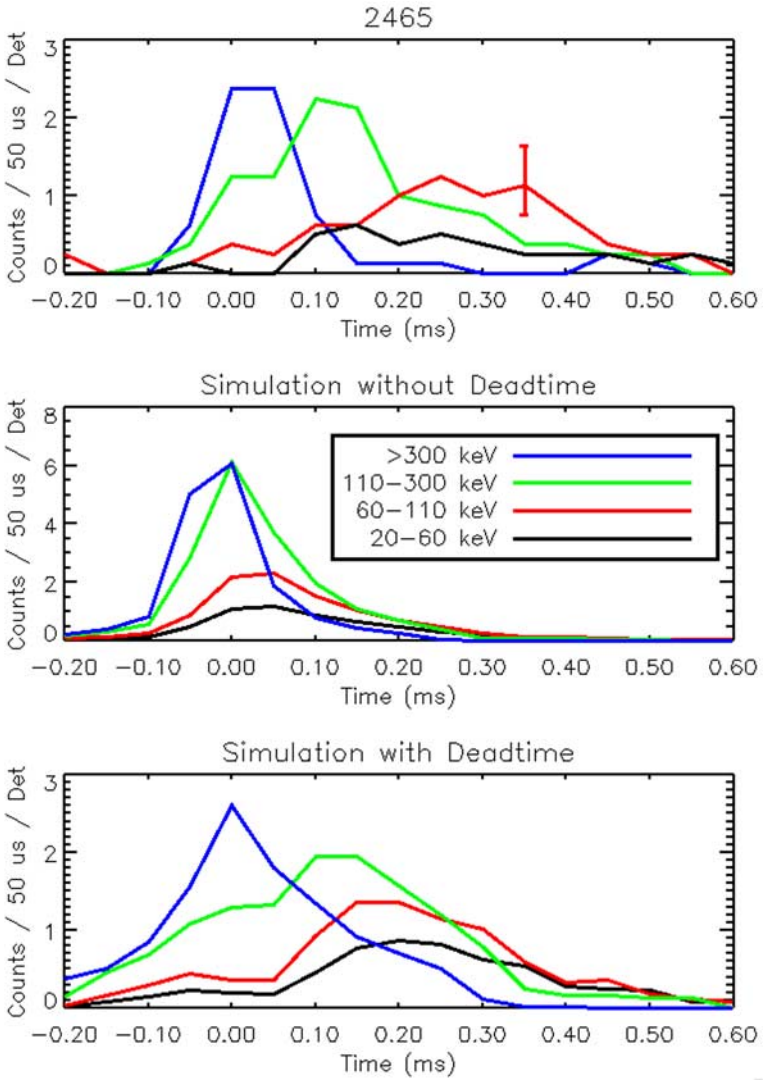

Figure 4. (top) Average over all eight LADs for BATSE Trigger 2465. Simulation (middle) without (note vertical scale has been allowed to expand) and (bottom) with the deadtime effect included.

successively larger annuli with ΔR of 15 km and collect the counts out to a limiting distance at which the flux through the outermost annulus has dropped by a factor of four from the flux through the innermost annulus. We remove the difference in light travel time for annuli at different distances by convolving the photons in each annulus with the RHESSI DRM and adjusting the time of arrival of each count to be relative to the average time of arrival of the hard counts. We then shift and add all of the annuli together and obtain a combined lightcurve for each simulation.

[19] Table 1 lists the limiting distance and the delay between the average time of arrival of the hard and soft components for all six of the simulations. Only the broad beams at 15 and 21 km produce time delays that are consistent with the RHESSI data. Figure 2 shows the RHESSI data along with a simulation of a broad beam at 15 km.

6. BATSE Tails

[20] Individual BATSE TGFs have been reported to show a much longer ($\approx$100 μs [*Feng et al.*, 2002]) delay than we find for the RHESSI data. We lack information about the location and brightness of individual events, so it is impossible to find a unique, quantitative fit to a particular BATSE TGF. However, if we consider the RHESSI events to be a representative of all TGFs, the limiting "brightest" and "dimmest" RHESSI peak count rates should allow us to find qualitatively comparable models.

[21] We limit ourselves to the choice of the broad, 15 km model since it is the only simulation that fits both the RHESSI timing and spectrum [*Dwyer and Smith*, 2005]. To generate a single simulated TGF we collect simulated photons in a 15 km distance range and scale the simulation so that the peak count rate is equivalent to either the bright or dim RHESSI case. The simulation is convolved with the front and rear BATSE DRMs to obtain count spectra for the front and rear detectors. Since the spectrum and brightness are different for the front and the rear detectors, we use equations (3) and (4) to apply the deadtime correction to each detector separately before taking their average.

[22] Figure 3 shows the results for the bright and dim simulations both before and after the deadtime correction

for a TGF located 200 km from the spacecraft. As can be seen, the primary effect of the deadtime has been to suppress the main, hard ($E_\gamma > 300$ keV) peak and overemphasize the soft ($E_\gamma < 300$ keV) Compton tail. This pushes apart the average arrival times of the hard and soft counts. Figure 4 shows a BATSE TGF along with a bright simulated TGF at a distance of 600 km both with and without the deadtime effect. The delay in the data is 160 ± 40 μs, while the delay in the simulation without deadtime is 70 μs and 130 μs with deadtime.

7. Summary and Discussion

[23] Our analysis of the time evolution of 431 RHESSI TGFs shows that there is a delay between the average arrival times of the hard and soft components of 28 ± 3 μs. We interpret this as the result of hard photons that are reprocessed to lower energies by Compton scattering in the atmosphere traveling a longer path than hard photons traveling directly to the spacecraft. We find that this delay is not consistent with models at a 30 km altitude, which agrees with the spectral result of *Dwyer and Smith* [2005]. This delay is also inconsistent with vertically oriented, narrowly beamed models at altitudes of 15 and 21 km. The only model that produces a long enough delay and also matches the RHESSI spectrum is the broadly beamed model at a 15 km altitude. We note that our analysis of the combined RHESSI data has averaged over whatever intrinsic variation there may be in the tilt and width of TGF beams and that, while the broad, 15 km model is empirically well-fit to the data, a physical motivation for the broad beam has yet to be obtained and will be the topic of future work.

[24] We have shown that the TGFs observed by BATSE suffer significant deadtime during the peak of the TGF. Once the deadtime effects have been included we can reproduce the long delay and low brightness seen by BATSE when using a broad, 15 km model scaled to match a RHESSI-like TGF. Our simple model underestimates the deadtime; a complete characterization of the LADs, including the long duration phosphorescence, would result in an a further suppression of the main peak and an increased delay between the hard and soft components.

[25] We believe that this effect, combined with the long (64 ms) trigger window of BATSE, allows the observed BATSE TGFs to be categorized into two groups: First, single peaked TGFs that are bright enough to be at, or near, the limiting brightness due to deadtime (such as BATSE trigger 2465). Since the Compton reprocessed tails from these events will also be bright, the TGFs will produce high measured count rates over a long period even if the main, hard peak is suppressed. Since TGFs that are farther away from BATSE have more pronounced Compton tails, this produces the interesting consequence that the ideal case for triggering BATSE is a very bright, distant TGF. Second, TGFs that are dim but anomalously long (such as BATSE triggers 7229 and 2221) as well as TGFs that contain several small peaks (such as BATSE triggers 8006 and 3813). In both of these cases the TGF can accumulate enough counts to trigger BATSE without significant deadtime.

[26] The majority of RHESSI-like TGFs, which are moderately bright, short, and single-peaked, would simply never have triggered BATSE. This is encouraging for upcoming instruments such as TARANIS and SPRITE-SAT that can now expect peak count rates ~4 times higher than would be predicted simply by scaling the BATSE fluxes down by detector area.

[27] **Acknowledgments.** This work was supported in part by the NSF grant ATM 0607885. We also wish to thank the anonymous reviewers for their comments and Thomas Gjesteland for noting an error in the original manuscript.

References

Bromm, V., and B. Shaefer (1999), The spectrum of GRB 930131 ("Superbowl Burst") from 20 keV to 200 MeV, *Astrophys. J.*, *520*, 661–665.

CERN Application Software Group (1993), GEANT—Detector description and simulation tool, *Tech. Rep. W5013*, CERN, Geneva, Switzerland.

Dwyer, J. R., and D. M. Smith (2005), A comparison between Monte Carlo simulations of runaway breakdown and terrestrial gamma-ray flash observations, *Geophys. Res. Lett.*, *32*, L22804, doi:10.1029/2005GL023848.

Feng, H., T. P. Li, M. Wu, M. Zha, and Q. Q. Zhu (2002), Temporal and spectral properties of gamma-ray flashes, *Geophys. Res. Lett.*, *29*(3), 1036, doi:10.1029/2001GL013992.

Fishman, G. J., et al. (1989), BATSE: The Burst and Transient Source Experiment on the Gamma Ray Observatory, paper presented at Gamma Ray Observatory Science Workshop, NASA Goddard Space Flight Center, Greenbelt, Md.

Fishman, G. J., et al. (1994), Discovery of intense gamma-ray flashes of atmospheric origin, *Science*, *264*, 1313–1316.

Humphreys, W. J. (1964), *Physics of Air*, 3rd ed., Dover, New York.

Knoll, G. F. (2000), *Radiation Detection and Measurement*, 3rd ed., John Wiley, New York.

Nemiroff, R. J., J. T. Bonnell, and J. P. Norris (1997), Temporal and spectral characteristics of terrestrial gamma ray flashes, *J. Geophys. Res.*, *102*(A5), 9659–9665.

Smith, D. M., et al. (2002), The RHESSI Spectrometer, *Sol. Phys.*, *210*, 33–60.

Smith, D. M., L. I. Lopez, R. P. Lin, and C. P. Barrington-Leigh (2005), Terrestrial gamma-ray flashes observed up to 20 MeV, *Science*, *307*, 1085–1088.

J. R. Dwyer, Department of Space Sciences, Florida Institute of Technology, Melbourne, FL 32901, USA.

G. J. Fishman, Department of Space Sciences, Florida Institute of Technology, Melbourne, FL 32901, USA.

B. W. Grefenstette and D. M. Smith, Santa Cruz Institute for Particle Physics, University of California, 1156 High Street, Santa Cruz, CA 95064, USA. (bwgref@scipp.ucsc.edu)